

Induced vortex dynamics in parallel Josephson junction arrays

Jinhyoung Lee, Jaejun Yu, and Gwangseo Park

Department of Physics, Sogang University, Seoul 121-742, Korea

(Received 27 June 1996)

As an attempt to understand many unusual characteristics of Josephson junctions between high- T_c Cu-oxide superconductors, we employed a parallel Josephson junction array model to study dynamical properties of the high- T_c superconducting single grain-boundary Josephson junction, where the relative scale of Josephson penetration depth λ_J is expected to play a crucial role in determination of its dynamics. Results of our numerical studies on the parallel Josephson junction arrays are presented for various values of Ginzburg-Landau parameters $\kappa_J = \lambda_J/a$, where a represents the array spacing. For the calculations, we take into account the full long-range inductions between vortices and the effects of induced magnetic fields by external currents in the array. From the results, it is found that subharmonic Shapiro steps emerge even under the zero external magnetic field for $\kappa_J \sim 1$, while subharmonic Shapiro steps are suppressed in the limits of either $\kappa_J \rightarrow 0$ or $\kappa_J \rightarrow \infty$. We conclude that, for the intermediate case of $\kappa_J \sim 1$, the edge magnetic fields induced by external currents may be responsible for the existence of subharmonic Shapiro steps with no external magnetic field present. [S0163-1829(97)01301-5]

I. INTRODUCTION

A collective motion of the ground state vortex lattice configurations has been attributed to the presence of fractional Shapiro steps in Josephson junction arrays under external magnetic fields.¹ Such interpretations arise from both numerical^{2,3} and analytic studies^{4,5} of the arrays of a resistively shunted junction (RSJ) model. Recently, however, subharmonic Shapiro steps were observed in experiments even when no magnetic fields were applied on Nb-Au-Nb Josephson junction arrays.⁶ In addition, Early *et al.* observed half-integral or third-integral Shapiro steps on grain-boundary junctions of biopitaxially grown $\text{YBa}_2\text{Cu}_3\text{O}_{7-\delta}$.⁷ And it was considered that such observed fractional Shapiro steps arise from trapped magnetic fields, which might enter into the junction from external sources during the experiment. On the other hand, from numerical simulations, it was suggested that subharmonic Shapiro steps could emerge in an inductive Josephson junction array model when the inductions between vortices and the effects of induced magnetic fields by external currents were taken into account.^{8,9} Despite many experiments and numerical studies, however, the origin of the subharmonic structures is still not clear yet.

In this paper, as an attempt to understand subharmonic Shapiro steps present in Josephson junctions of high- T_c superconductors, we employed a parallel Josephson junction array model to study dynamical properties of the high- T_c single grain-boundary Josephson junction, where the relative scale of Josephson penetration depth λ_J is expected to play a crucial role in determination of its dynamics. We presented results of our numerical studies on the parallel Josephson junction arrays for various values of Ginzburg-Landau parameters $\kappa_J = \lambda_J/a$, with a being an array spacing, where the full long-range inductions between vortices and the effects of induced magnetic fields by external currents are taken into account. From the results, we found that onset currents at which voltages develop take their minimum values for $\kappa_J \sim 1$ and also subharmonic Shapiro steps emerge for

$\kappa_J \sim 1$ even under a zero external magnetic field, while subharmonic Shapiro steps are suppressed in the limits of either $\kappa_J \rightarrow 0$ or $\kappa_J \rightarrow \infty$. Therefore, we conclude that, for the intermediate case of $\kappa_J \sim 1$, edge magnetic fields induced by the external current may be responsible for the existence of subharmonic Shapiro steps with no external magnetic field present.

In Sec. II, we will briefly review the inductive Josephson junction array model within the context of the resistively shunted junction model where inductions by local currents are included. In Sec. III, we present the results of parallel Josephson junction arrays modeled on high- T_c single grain-boundary Josephson junctions. Even though we included full inductions in our models, the unusual behaviors of high- T_c Josephson junctions are found to be correlated with edge magnetic fields. Considering the effects of edge magnetic inductions, we suggest an analytic approach to the inductive Josephson junction array model for the intermediate case of $\kappa_J \sim 1$ in Sec. IV. Finally we conclude with a summary in Sec. V.

II. METHOD

Let us consider an $(M \times N)$ array of weakly coupled Josephson junctions, which are characterized by the coupling constants such as critical current $I_\mu^c(r)$ and resistance $R_\mu(r)$ between superconducting grains at site r and site $r + \mu$ with a lattice displacement $\mu = \hat{x}, \hat{y}$. (Here we use the formalism and notation adopted in the Ref. 8.) Then, the current along the μ direction from site r is

$$I_\mu(r, t) = I_\mu^c(r) \sin\{\Delta_\mu \theta(r, t) - A_\mu(r, t)\} + \frac{\Phi_0}{2\pi R_\mu(r)} \frac{d}{dt} \{\Delta_\mu \theta(r, t) - A_\mu(r, t)\}, \quad (1)$$

where $\Delta_\mu \theta(r) = \theta(r + \mu) - \theta(r)$ and $A_\mu(r) = (2\pi/\Phi_0) \int_r^{r+\mu} \mathbf{A} \cdot d\mathbf{r}$. Because it is convenient to describe

the system in terms of the plaquette variables, we have from current conservation that

$$\begin{aligned} I_x(r,t) &= J(R,t) - J(R - \hat{y}, t) + I_{\text{ext}}(t), \\ I_y(r,t) &= J(R - \hat{x}, t) - J(R,t), \end{aligned} \quad (2)$$

where $J(R,t)$ is the loop current on the plaquette R , defined to be positive for current flowing in the counterclockwise direction. We may rewrite these equations in a shorthand notation

$$I_\mu(r,t) = \Delta_\mu \times J(R,t) + \delta_{\mu x} I_{\text{ext}}(t). \quad (3)$$

When current exists in the Josephson junction array, it induces magnetic fields. Thus, the total magnetic flux at the plaquette R is given by a sum of the external and induced magnetic flux,

$$\Phi(R,t) = \Phi_{\text{ext}} + \sum_{R'} L(R,R') J(R',t) + E(R) I_{\text{ext}}(t), \quad (4)$$

where $L(R,R')$ is the inductance matrix¹⁰ due to the plaquette current $J(R',t)$, and $E(R)$, the inductance by the external current $I_{\text{ext}}(t)$. The last term on right-hand side of Eq. (4), which is called edge magnetic fields, has its maximum amplitude at the edges of the array and decreases towards its center.

Since the equations of motion are gauge invariant, we can replace $[\Delta_\mu \theta(r,t) - A_\mu(r,t)]$ by $\Psi_\mu(r,t)$ so that the Langevin dynamical equation of motion can be written in terms of $\Psi_\mu(r,t)$, from Eqs. (1), (3), and (4),

$$\begin{aligned} \frac{\Phi_0}{2\pi} \frac{1}{R_\mu(r)} \frac{d}{dt} \Psi_\mu(r,t) &= -I_\mu^c(r) \sin \Psi_\mu(r,t) + \delta_{\mu x} I_{\text{ext}}(t) \\ &\quad - \frac{\Phi_0}{2\pi} \Delta_\mu \times \sum_{R'} L^{-1}(R,R') \\ &\quad \times \left\{ \Delta_\mu \times \Psi_\mu(r',t) + \frac{2\pi}{\Phi_0} \Phi_{\text{ext}} \right. \\ &\quad \left. + \frac{2\pi}{\Phi_0} E(R') I_{\text{ext}}(t) \right\}, \end{aligned} \quad (5)$$

and the total flux $\Phi(R,t)$ can be acquired by curling the $\Psi_\mu(r,t)$,

$$\begin{aligned} -\frac{2\pi\Phi(R,t)}{\Phi_0} &= \Psi_x(r,t) + \Psi_y(r+x,t) - \Psi_x(r+y,t) \\ &\quad - \Psi_y(r,t) = \Delta_\mu \times \Psi_\mu(r,t). \end{aligned} \quad (6)$$

In a regular-ordered Josephson junction array, there is only a single critical current I_0^c and resistance R_0 . On the other hand, in a disordered array of Josephson junctions, we may have a random distribution of critical currents and shunted resistances.¹¹ But instead of having a purely random distribution, we may consider a Gaussian distribution of $\{I_\mu^c(r)\}$ and $\{R_\mu(r)\}$ with their averages equal to I_0^c and R_0 , respectively, assuming the probability distributions

$$P(Q_\mu(r)) = [2\pi(\Delta Q)^2]^{-1/2} \exp\left[-\frac{[Q_\mu(r) - Q_0]^2}{2(\Delta Q)^2}\right], \quad (7)$$

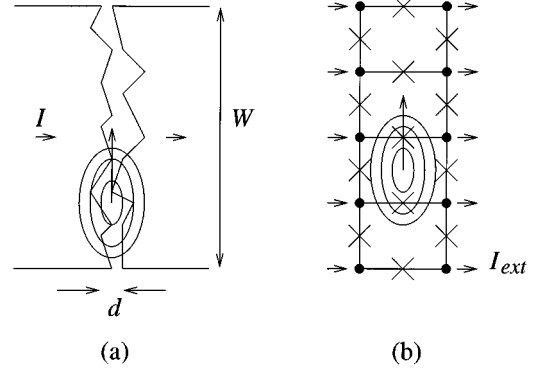


FIG. 1. (a) Schematic drawing of a high- T_c single grain-boundary Josephson junction. W is the width and d the separation of the junction interface. The ellipses represent the magnetic vortex. (b) A parallel Josephson junction array modeled as a single grain-boundary Josephson junction.

where $\{Q_\mu(r)\}$ represents either $\{I_\mu^c(r)\}$ or $\{R_\mu(r)\}$, Q_0 its average value and ΔQ the standard deviation.

By normalizing the time as $\tilde{t} = t/\tau_c$ with $\tau_c \equiv 1/\nu_c \equiv \Phi_0/2\pi I_0^c R_0$, the current as $\tilde{I}_\mu(r) = I_\mu(r)/I_0^c$, the resistance as $\tilde{R}_\mu(r) = R_\mu(r)/R_0$, the voltage as $\tilde{V}_\mu(r) = V_\mu(r)/(I_0^c R_0)$, the flux as $\tilde{\Phi}(R) = 2\pi\Phi(R)/\Phi_0$, $\tilde{L}(R,R') = L(R,R')/(\mu_0 a)$, and $\tilde{E}(R) = 2\pi E(R)I_0^c/\Phi_0$, Eq. (5) can be rewritten as

$$\begin{aligned} \frac{1}{\nu_c \tilde{R}_\mu(r)} \frac{d}{dt} \Psi_\mu(r,t) &= -\tilde{I}_\mu^c(r) \sin \Psi_\mu(r,t) + \delta_{\mu x} \tilde{I}_{\text{ext}}(t) \\ &\quad - \kappa^2 \Delta_\mu \times \sum_{R'} \tilde{L}^{-1}(R,R') \\ &\quad \times \left\{ \Delta_\mu \times \Psi_\mu(r',t) + \tilde{\Phi}_{\text{ext}} \right. \\ &\quad \left. + \tilde{E}(R') \tilde{I}_{\text{ext}}(t) \right\}, \end{aligned} \quad (8)$$

where $\kappa \equiv (2\pi\mu_0 a I_0^c/\Phi_0)^{-1/2}$. It is noted that, for the diagonal inductive matrix $L(R,R')$, κ becomes $\kappa_J = \lambda_J/a$, i.e., the ratio of the Josephson penetration depth λ_J to lattice constant a . Then, since the off-diagonal terms of $L(R,R')$ drop off rapidly, κ can be approximated by κ_J .

III. SINGLE LONG JOSEPHSON JUNCTION

Now, consider a weakly coupled single high- T_c grain-boundary junction, where the separation d of the junction interface is comparable to the coherence length ξ and the junction width W is much larger than the coherence length ξ of the high- T_c superconducting junctions with a large variation of Josephson penetration depth λ_J . Due to the complicated interfacial structure of the high- T_c grain boundary, it is expected to have a large variation of local junction characteristics, e.g., effective separations. As shown in Fig. 1, due to a short coherence length, there may exist many microscopic local junctions within a single grain-boundary junction. Since the stronger couplings induce larger critical currents, most of the current will be carried through local junctions with the stronger couplings. Hence, it is reasonable to assume that a single grain-boundary junction consists of

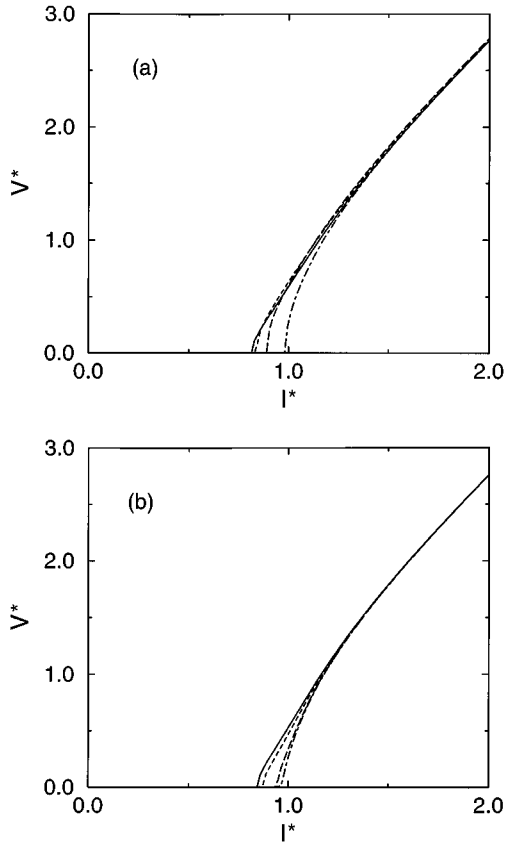


FIG. 2. Zero-field I - V characteristics of dc-driven (2×11) parallel Josephson junction array. The horizontal axis is \tilde{I}_{dc} and the vertical axis is the time-averaged voltage. Each I - V curve is calculated (a) for $1/\kappa^2=0.1$ (dot-dashed line), $1/\kappa^2=0.5$ (long dashed line), $1/\kappa^2=1.0$ (dashed line), and $1/\kappa^2=1.5$ (solid line), respectively, from right to left and (b) for $1/\kappa^2=2.0$ (solid line), $1/\kappa^2=2.5$ (dashed line), $1/\kappa^2=5.0$ (long dashed line), and $1/\kappa^2=10.0$ (dot-dashed line), respectively, from left to right.

multiple local junctions, where each superconducting domains are coupled with the relatively stronger Josephson couplings. With these assumptions, we can model the high- T_c single grain-boundary junction by an array of parallel Josephson junctions with various Josephson couplings.

In order to study the unusual dynamic behaviors of the high- T_c single grain-boundary junctions under no external magnetic field, we consider a model of the (2×11) parallel Josephson junction array shown in Fig. 1. To simulate the superconducting domains as strongly coupled Josephson junctions, we take the critical current I_y^c to be 10 times the critical current I_x^c and the resistance R_y to be one-tenth of the resistance R_x , respectively. The typical regular distributions of couplings are taken to be $I_x^c=I_0$, $I_y^c=10I_0$, $R_x=R_0$, and $R_y=R_0/10$ for various sizes of the vortex for the given junction separation a , i.e., κ 's. When the size of a vortex becomes comparable to that of a plaquette, the vortex is affected by the local properties of the array. On the other hand, the vortex will experience the global average when the single vortex covers almost the whole size of the array. The vortex dynamics can be quite different, depending on the relative size of vortices and plaquettes.

In Fig. 2, we present the results of I - V characteristics

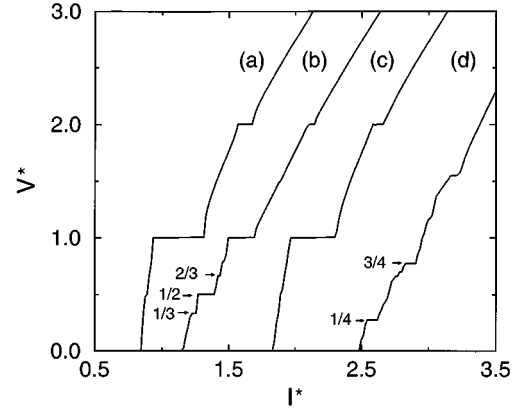


FIG. 3. Zero-field I - V characteristics of ac-driven (2×11) parallel Josephson junction array, $\tilde{\nu}_{ac}=2\pi/10$, $\tilde{\Phi}_{ext}=0$, $\tilde{I}_{ac}=0.5\tilde{I}_0^c$. (a) $1/\kappa^2=0.1$, (b) $1/\kappa^2=1.5$, and (c) $1/\kappa^2=10.0$. In addition, we include the result of (d) $1/\kappa^2=1.5$ for the irregular distribution of I_c and R with $\Delta I_c=0.3$ and $\Delta V_J=0$. Successive curves are displaced along the horizontal axis by 0.5 units.

calculated on the various values of κ where only direct (dc) currents are applied. As shown in Fig. 2, it is found that the onset currents change with respect to the change of κ . The onset current becomes the smallest at $1/\kappa^2 \approx 1/\kappa_0^2 = 1.5$. But the onset current approaches I_0 as κ deviates away from κ_0 . Since the sliding of induced magnetic vortices contributes to the development of voltage in addition to the normal currents, it is obvious that the voltage onset occurs with the external currents I_{ext} being smaller than the original I_0 , i.e., $I_{ext} < I_0$. The results on the change of the onset currents imply that the motion of the induced vortex is important in the case that the size of the vortex is comparable to that of the plaquette, i.e., $\kappa \sim \kappa_0$, while it becomes less important at either $\kappa \rightarrow 0$ or $\kappa \rightarrow \infty$.

In Fig. 3, when ac currents are driven together with dc current, the I - V characteristics are calculated and found to have the appearance of subharmonic Shapiro steps at various values of κ . The widths of integral Shapiro steps are a little affected by even large changes of κ . On the other hand, the $1/2$ and $1/3$ subharmonic Shapiro steps become the largest at $\kappa \sim \kappa_0$ as shown in Fig. 3(b), while they are suppressed in the limits of either $\kappa \rightarrow 0$ or $\kappa \rightarrow \infty$ as shown in Figs. 3(a) and 3(c). Our present results, showing that subharmonic Shapiro steps become large at $\kappa \rightarrow \kappa_0$, are consistent with recent experiments by Early *et al.*,⁷ where the κ values were estimated to be roughly order of 1.

In addition to the effects of induced magnetic fields by vortices as well as by external currents, an irregular distribution of Josephson couplings can be considered as another important factor determining the I - V characteristics of Josephson junction arrays. In our previous work,¹¹ we have considered an irregular distribution of couplings in a model for the high- T_c granular junction, in order to examine the effects of translational symmetry breaking. In the current study, as an example of showing the effects of disorder, we have chosen a particular case of the standard deviation of critical currents, ΔI_c , to be 0.3 and the deviation of Josephson voltage, ΔV_J , to be zero.¹³ The general features found in the I - V characteristics of irregular distributions are quite

similar to those of the regular ones. Although there is no major difference in the overall shape, however, unusual distinctive features in the I - V curve emerge from the Josephson junction arrays with the irregular distribution as shown in Fig. 3(d). In fact, the clear appearance of the 1/4 steps in the calculated I - V curves is extremely interesting, as such 1/4 steps have not been observed either experimentally or theoretically for the case of the regular Josephson arrays with no external field present. Thus, the irregular distribution is considered to be responsible for the appearance of the 1/4 steps in the I - V characteristics.

Although the induced vortex dynamics are the primary reason for the existence of subharmonic Shapiro steps, however, the irregular distributions of Josephson couplings can further complicate the I - V characteristics of the Josephson junction arrays or the high- T_c grain-boundary junction, as discussed in the present work. Moreover, it is observed that there exist strong correlations among the widths of half and integral steps, and 1/3 or 1/4 steps, depending on variations of the parameter κ as well as on the degree of disorder in the distributions. Similar observations were reported in experiments⁷ and numerical calculations,¹² where the half-integer Shapiro steps were found to be correlated with the integral Shapiro steps in which, for instance, the larger the width of the half steps, the smaller that of the integral steps. In our calculations, we found that the widths of 1/4 steps are correlated with those of half or integral steps just as for the case of the half and integral steps in the regular distributions.

IV. EDGE MAGNETIC FIELD

In the previous section, we discussed the numerical results on the arrays of inductive parallel Josephson junctions, which are modeled for the high- T_c single grain-boundary Josephson junction. The two most important observations are that (a) induced vortex dynamics can be neglected in the limits of either $\kappa \rightarrow 0$ or $\kappa \rightarrow \infty$ and (b) subharmonic Shapiro steps emerge due to induced vortex dynamics at $\kappa \rightarrow \kappa_0$ under no externally applied magnetic field. In this section, we shall discuss some aspects of analytic investigations.

First, let us consider the limit of $\kappa \rightarrow 0$, where the magnetic fields fully vanish by screening currents. Since the inductive current term is negligible, Eq. (8) can be reduced to the equations of noncoupled single junctions,

$$-\frac{1}{v_c \tilde{R}_\mu(r)} \frac{d}{dt} \Psi_\mu(r, t) = \tilde{I}_\mu^c(r) \sin \Psi_\mu(r, t) - \delta_{\mu x} \tilde{I}_{\text{ext}}(t). \quad (9)$$

The limit of $\kappa \approx \lambda_J/a \rightarrow 0$ corresponds to the case that the range of the induction of vortices becomes zero. Thus, it implies that the dynamics of vortices cannot have any correlation even between the nearest-neighbor junctions. In the limit of $\kappa \rightarrow \infty$, however, in contrast, the correlation between junctions even far from each other becomes very strong so that the junctions are locked collectively as the induction range becomes large. From Ampère's law, the total sum, over the whole array, of the inductive local magnetic flux on each plaquette should be zero without any external magnetic field. In this limit, a single vortex can cover the whole array and the local magnetic flux of this single vortex is positively

proportional to the total flux. Hence, the local magnetic flux is nearly zero and the magnetic inductions can be neglected. Thus, Eqs. (1), (3), and (4) is reduced to the equation of a noninductive Josephson junction array,

$$\begin{aligned} \tilde{I}_\mu(r, t) &= \tilde{I}_\mu^c(r) \sin\{\Delta_\mu \theta(r, t) - A_\mu^{\text{ext}}\} \\ &\quad + \frac{1}{v_c \tilde{R}_\mu(r)} \frac{d}{dt} \{\Delta_\mu \theta(r, t)\}, \\ \Delta_\mu \cdot \tilde{I}_\mu(r, t) &= \tilde{I}_{\text{ext}}(t). \end{aligned} \quad (10)$$

In these two limiting cases, we obtained the noncoupled and noninductive Josephson junction equations, respectively. Therefore, these results illustrate that there is no subharmonic structure present for the limits of either $\kappa \rightarrow 0$ or $\kappa \rightarrow \infty$.

Before considering the intermediate case of $\kappa \sim 1$, let us imagine a fully translationally symmetric Josephson junction array with full inductions present among vortices. When no external magnetic field is applied, there is no instantaneous screening current and no magnetic field can be induced by currents due to the translational symmetry. Thus, no vortex dynamics is possible in the translationally symmetric Josephson junction array. On the other hand, when we consider the nonsymmetric, finite-width Josephson junction array, the magnetic fields are induced around the edge of the array by external currents. Thus, for the intermediate case of $\kappa \sim 1$, we may conjecture that the edge magnetic fields are crucial factors for understanding of behaviors of inductive Josephson junction arrays. The effects of screening currents can be considered perturbatively with an undetermined parameter. Then, the total flux is approximated to

$$\Phi(R, t) \approx (1 - \gamma) \Phi_{\text{dc}}(R) + (1 - \gamma) \Phi_{\text{ac}}(R) \cos \omega_{\text{ac}} t, \quad (11)$$

where $\Phi_{\text{dc}}(R) = \Phi_{\text{ext}} + E(R) I_{\text{dc}}$, $\Phi_{\text{ac}}(R) = E(R) I_{\text{ac}}$, γ is the positive small parameter indicating screening effects, and the instantaneous voltage is given by

$$\frac{\Phi_0}{2\pi} \frac{d}{dt} \Psi_\mu(r, t) = \frac{\Phi_0}{2\pi} \frac{d}{dt} \Delta_\mu \theta(r, t) + \frac{\Phi_0}{2\pi} A_\mu^{\text{ac}}(r) \omega_{\text{ac}} \sin \omega_{\text{ac}} t, \quad (12)$$

with $(1 - \gamma) \Phi_{\text{dc}}(R) = \Delta_\mu \times A_\mu^{\text{dc}}(r)$ and $(1 - \gamma) \Phi_{\text{ac}}(R) = \Delta_\mu \times A_\mu^{\text{ac}}(r)$. Now, Eq. (5) can be rewritten as the equations of perturbatively inductive Josephson junction arrays with the total flux $\Phi(R, t)$ as an external magnetic flux,

$$\begin{aligned} I_\mu(r, t) &= I_\mu^c(r) \sin\{\Delta_\mu \theta(r, t) - A_\mu^0(r) - A_\mu^{\text{ac}}(r) \cos \omega_{\text{ac}} t\} \\ &\quad + \frac{\Phi_0}{2\pi} \frac{1}{R_\mu(r)} \frac{d}{dt} \Delta_\mu \theta(r, t) + \frac{\Phi_0}{2\pi} \frac{A_\mu^{\text{ac}}(r)}{R_\mu(r)} \omega_{\text{ac}} \sin \omega_{\text{ac}} t, \\ \Delta_\mu \cdot I_\mu(r, t) &= I_{\text{ext}}(t). \end{aligned} \quad (13)$$

Note that the last term of the currents is the normal currents driven by the total magnetic flux and it can be treated as the renormalization of the external current I_{ext} . Since the oscillating vector potential in Eq. (13) makes it difficult to be analytically solved, we may consider two limiting cases.

In the high-voltage limit of $\omega_J \gg \omega_{\text{ac}}$ with $\omega_J = (2\pi/\Phi_0) \langle V(t) \rangle_t$, the total magnetic flux $\Phi(R, t)$ varies

slowly in the time scale of $2\pi/\omega_J$ and it can be approximated to be the time-independent magnetic flux $\Phi(R, \tau)$ for the time interval of $t \ll \tau \sim 2\pi/\omega_{ac}$. One can solve analytically Eq. (13) with this magnetic flux $\Phi(R, \tau)$ by selecting the proper gauge.⁵ Then the obtained quantities need to be averaged with respect to τ . In the low-voltage limit of $\omega_J \ll \omega_{ac}$, the total magnetic flux $\Phi(R, t)$ varies so fast that the system experiences the averaged magnetic flux $\Phi_{dc}(R)$ while the dissipation by the dynamics of vortices becomes large. By renormalizing the external currents with the normal currents driven by the total magnetic flux, these equations can be solved with the averaged magnetic flux $\Phi_{dc}(R)$.⁵ Here the total magnetic flux $\Phi(R)$ simply becomes $\Phi_{ext} + E(R)I_{dc}$ and $\Phi(R)$ is directly proportional to I_{dc} when no external magnetic flux is applied. It is expected that, if the $1/2$ step occurs at $I = I_{1/2}$, the $1/n$ step will emerge near $(2/n)I_{1/2}$ due to the linearity of the total flux on I_{dc} . The effects of screening the magnetic flux can be analyzed by the nonzero γ . These screening currents will affect the behaviors of Josephson junction arrays, for example, the widths of the Shapiro steps.

V. CONCLUSIONS

We modeled the high- T_c single grain-boundary Josephson junctions by parallel Josephson junction arrays. From our numerical studies, it is shown that the subharmonic Shapiro steps can emerge even without any external magnetic fields,

due to the induced magnetic fields by local currents. For $\kappa \sim 1$, the dynamics of induced vortices play a crucial role in the unusual behaviors of parallel Josephson junction arrays. On the other hand, for the limits of either $\kappa \rightarrow 0$ or $\kappa \rightarrow \infty$, the dynamics of induced vortices is less important in self-radiation and subharmonic Shapiro steps. By conjecturing that the edge magnetic flux is a crucial factor in understanding the unusual behaviors of Josephson junction arrays, we presented the results of an analysis on the inductive Josephson junction array model by considering the perturbative limits of the edge magnetic fields as external magnetic fields. As a result, in the low-voltage limit of $\omega_J \ll \omega_{ac}$, it is predicted that the $1/n$ Shapiro step may emerge near the $2/n$ value of the current for the $1/2$ Shapiro step. For further details, we need to perform a further analysis of the screening currents and edge magnetic fields. An analytical study of perturbatively inductive Josephson junction arrays is in progress.

ACKNOWLEDGMENTS

We are grateful to Professor H.C. Lee and Dr. K. Char for helpful discussions. This work was supported by the Ministry of Science and Technology of Korea through the HTRSA. J.Y. acknowledges the support by the Basic Science Research Institute program, Ministry of Education, Project No. 95-2414.

¹S.P. Benz, M.S. Rzchowski, M. Tinkham, and C.J. Lobb, Phys. Rev. Lett. **64**, 693 (1990).
²J.U. Free, S.P. Benz, M.S. Rzchowski, M. Tinkham, C.J. Lobb, and M. Octavio, Phys. Rev. B **41**, 7267 (1990).
³K.H. Lee, D. Stroud, and J.S. Chung, Phys. Rev. Lett. **64**, 692 (1990).
⁴M.Y. Choi, Phys. Rev. B **46**, 564 (1992).
⁵Italo F. Marino and Thomas C. Halsey, Phys. Rev. B **50**, 6289 (1994); Italo F. Marino (unpublished).
⁶H.C. Lee, R.S. Newrock, D.B. Mast, S.E. Hebboul, J.C. Garland, and C.J. Lobb, Phys. Rev. B **44**, 921 (1991); S.E. Hebboul and J.C. Garland, *ibid.* **47**, 5190 (1993).
⁷E.A. Early, R.L. Steiner, A.F. Clark, and K. Char, Phys. Rev. B **50**, 9409 (1994).

⁸D. Domínguez and Jorge V. José, Phys. Rev. Lett. **69**, 514 (1992); Int. J. Mod. Phys. B **8**, 3749 (1994).
⁹J.R. Phillips, H.S.J. van der Zant, J. White, and T.P. Orlando, Phys. Rev. B **50**, 9387 (1994).
¹⁰R.W. King, in *Handbuch der Physik*, edited by S. Flügge (Springer-Verlag, Berlin, 1958), Vol. XVI, p. 197.
¹¹Jinhyoung Lee, Sangmin Lee, Jaejun Yu, and Gwangseo Park, Phys. Rev. B **53**, 3578 (1996).
¹²M.S. Rzchowski, L.L. Sohn, and M. Tinkham, Phys. Rev. B **43**, 8682 (1991); M. Octavio, J.U. Free, S.P. Benz, R.S. Newrock, D.B. Mast, and C.J. Lobb, *ibid.* **44**, 4601 (1991).
¹³This correlation, $\Delta V_J = 0$, of the critical currents and shunted resistance is often observed in granular high- T_c bridge junctions (Ref. 11) and high- T_c grain boundary junctions (Ref. 7).